Available online at www.sciencedirect.com

ScienceDirect

Procedia IUTAM 15 (2015) 34 – 40

Procedia IUTAM

www.elsevier.com/locate/procedia

IUTAM Symposium on Multiphase flows with phase change: challenges and opportunities, Hyderabad, India (December 08 – December 11, 2014)

Turbulent Transport Processes at Rough Surfaces with Geophysical Applications

Srikanth Toppaladoddi[a,b], Sauro Succi[c], John S. Wettlaufer[a,b,]

[a]*Mathematical Institute, University of Oxford, Oxford OX2 6GG, United Kingdom*
[b]*Yale University, New Haven, Connecticut 06520-8109, USA*
[c]*Istituto Applicazioni Calcolo "Mauro Picone", C.N.R., Rome 00185, Italy*

Abstract

In this numerical study we use the Lattice Boltzmann Method to investigate the effects of periodic and randomly rough surfaces on the turbulent transport of momentum and heat. A two-dimensional MPI code has been developed and validated against many test cases. We examine in some detail Rayleigh-Benárd convection in the presence of rough walls and study the effects of the wavelength and amplitude of the roughness distribution on the flow.

Peer-review under responsibility of Indian Institute of Technology, Hyderabad.

Keywords: Turbulence, rough surfaces, sea ice;

1. Introduction

The recent decline in the Arctic sea-ice extent has triggered debates on climate change and its implications for humanity. A range of observations have shown a decrease both in the areal extent and the average thickness of Arctic sea ice. For example, in the central Arctic, the average sea-ice thickness has decreased by approximately 44 %[1]. Given the complexity and the coupling of the various subsystems of the Arctic climate, there could be many factors responsible for this decline. One of the factors whose contribution is relatively poorly understood is the turbulent heat flux from the ocean to the underside of the ice. Though the climatological thickness of sea ice has been found to be very sensitive to the oceanic heat flux in theoretical models[2], broad scale systematic observational studies are challenging[3] and typical closure schemes in Global Climate Models (GCMs) are unreliable as can be understood from recent laboratory experiments[4].

As an initial step towards addressing this issue, we investigate the effects of a rough surface (a) with a periodic structure and (b) whose spectral properties are the same as that of Arctic sea ice, on a turbulent flow. This is done using the Lattice Boltzmann Method (LBM) which offers many advantages over the traditional Navier-Stokes solvers. One of the primary aims of this study is to understand how the turbulent fluxes are affected by the roughness of the

E-mail address: john.wettlaufer@yale.edu

Peer-review under responsibility of Indian Institute of Technology, Hyderabad.
doi:10.1016/j.piutam.2015.04.006

surface, and how this, in turn, affects the melting/growth of the sea ice at the ice-ocean interface. Before addressing this challenging latter aspect of phase change, we begin by studying a stationary rough surface.

2. The Lattice Boltzmann Method

The Lattice Boltzmann Method is derived from Boltzmann's kinetic theory as follows. Because the Boltzmann equation describes the time evolution for a single particle distribution function, various moments of the distribution function give the appropriate macroscopic fields like density, velocity, and temperature. One can simplify the Boltzmann equation[5,6], which is an integro-differential equation that is quadratic in the distribution function, by replacing the integral with a linear term, known as the BGK-W collision term (named after Bhatnagar, Gross, Krook, and Welander). Although the collision term in this approximation is linear, the nonlinearity is "hidden" in the equilibrium distribution function. In the original equation, the particles travel in and infinite number of directions with constant velocities, but these directions must be truncated for computation purposes, and it was shown by Frisch, Pomeau & Hasslacher that in two dimensions a minimum of seven velocity directions, with symmetry, is required to recover the Navier-Stokes Equations (NSE) from the Lattice Boltzmann equation (LBE)[7].

There are several advantages to solving the LBE rather than the NSE, which include:

(1.) The flow is weakly compressible in the LBM, and hence pressure is a local quantity.
(2.) The streaming operation is exact.
(3.) LBM can handle complex geometries more naturally and efficiently.
(4.) LBM is not just for fluid flows. Physical processes like phase transitions can be included in the full simulation[7]. (This is advantageous as we plan to study sea ice growth and its interaction with the oceanic turbulent flow[8])

The LBE, with the BGK approximation, is written as:

$$f_i(\underline{x} + \underline{c_i}\Delta t, t + \Delta t) = f_i(\underline{x}, t) - \frac{\Delta t}{\tau}(f_i - f_i^{eq}); \quad i = 0, 1, 2, ..., 8, \tag{1}$$

where f_i are the non-equilibrium distribution functions, f_i^{eq} are the equilibrium distribution functions, $\underline{x}$ is the position vector, $\underline{c_i}$ are the constant particle velocities, Δt is the time step, and τ is the collision time-scale.

For the present study we use the D2Q9 model (D = 2 denoting 2 dimensions and Q = 9 denoting 9 velocities). The form of f_i^{eq} is crucial for the recovery of the NSE, which is obtained in the limit of low Mach numbers, where $Ma \equiv u/c_s$ is the Mach number, u is the macroscopic fluid speed and c_s is the speed of sound. In the Boltzmann kinetic theory f^{eq} is a Gaussian but, in the numerical model, terms only up to $O(Ma^2)$ are retained. The truncated form of f_i^{eq} used in this model is given by:

$$f_i^{eq} = \rho w_i \left[1 + \frac{\mathbf{c_i}.\mathbf{u}}{c_s^2} + \frac{(\mathbf{c_i}.\mathbf{u})^2}{2c_s^4} - \frac{u^2}{2c_s^2}\right]. \tag{2}$$

Here, w_i are the weights for different directions, $c = \Delta x/\Delta t$ and $c_s = c/\sqrt{3}$.

The NSE can be recovered from the LBE by carrying out a multiple-scale analysis, considering the small Knudsen number (the ratio of the mean free path of a molecule to the largest length scale in the problem) limit[5]. The form of kinematic viscosity is obtained from this expansion, and is given by $\nu = c_s^2\left(\tau - \frac{\Delta t}{2}\right)$. In lattice units $\Delta x = \Delta t = 1$, and hence the scheme develops numerical instabilities as $\tau \to 0.5^+$.

Finally, once the f_i are calculated, the macroscopic fields are obtained from the following equations:

$$\rho = \sum_{i=0}^{8} f_i; \qquad \rho\underline{u} = \sum_{i=0}^{8} f_i\underline{c_i}. \tag{3}$$

3. Validation

We have developed a two-dimensional, MPI parallelized LB code to study the flow effects of rough surface in two dimensions. The code has been extensively validated, and we discuss some of the validation cases here:

1. *Channel flow in two-dimensions*
The canonical geometries in the study of wall-bounded turbulent flows are pipes and channels[9]. Given the simple geometry, we test our code to study transitional flow in two-dimensional (2D) channels. The flow is forced using a constant pressure gradient along the channel, with a no-slip condition at the top and bottom walls and periodic conditions along its length. In our simulations the pressure gradient is constant, so the velocity scale is chosen to be $u_0 = |\nabla p| L^2/\rho\nu$, where $|\nabla p|$ is the pressure gradient, L is the half-channel width, ρ and ν are the density and kinematic viscosity of the fluid, and hence the pressure Reynolds number (Re_p) is defined as $Re_p = |\nabla p| L^3/2\rho\nu^2$. The solution can be represented as $\mathbf{u}(\mathbf{x}, t) = U_0(z)\mathbf{i} + \mathbf{v}(\mathbf{x}, t)$, where $\mathbf{u}(\mathbf{x}, t)$ is the total velocity field, $U_0(z) = \left(1 - z^2\right)$ is the Poiseuille velocity profile, $\mathbf{i}$ is the unit vector along the channel, and $\mathbf{v} = (v_x, v_z)$ is the departure from $U_0(z)\mathbf{i}$. Another quantity of interest is the flux rate, $\Delta Q = \left\langle \int_{-1}^{1} v_x dz \right\rangle$, where $\langle \ldots \rangle$ denotes horizontal averaging.
Figure (1a) shows the time variation of ΔQ for $Re_p = 2935$ and $\alpha_0 = 0.3387$, where α_0 is the minimal wavenumber of the imposed disturbance. Because the pressure gradient is constant, the flow rate decreases before reaching a steady state value of -0.088, which is close to -0.072 obtained by Rozhdestvensky & Simakin using spectral methods[10]. Figure (1b) shows the the temporal behaviour of (v_x, v_z) once the flow has reached a statistically steady state. The results obtained are in good agreement with the findings of Rozhdestvensky & Simakin.

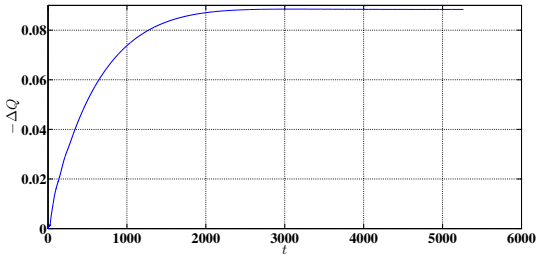

(a) Time variation of ΔQ for $Re_p = 2935$ and $\alpha_0 = 0.3387$.

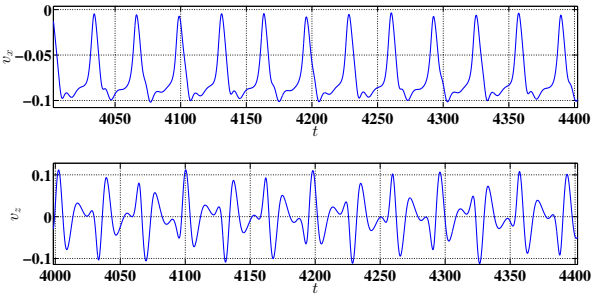

(b) Time variation of v_x and v_z at $(x, z) = (0, 0)$ for $Re_p = 2935$ and $\alpha_0 = 0.3387$.

Fig. 1: Validation for 2D channel flow. Comparison with Rozhdestvensky & Simakin[10] who used spectral methods.

2. *Rayleigh-Benárd convection in two dimensions*
The classical problem of Rayleigh-Benárd convection involves the transport of heat by convection when a critical Rayleigh number (Ra) is exceeded. Two horizontal walls are maintained at different temperatures – the bottom wall is maintained at a temperature $T_0 + \Delta T$ and the upper wall is maintained at a temperature T_0 – separated by a vertical distance H. The kinematic viscosity and the thermal diffusivity of the fluid are ν and κ respectively, and β is the co-efficient of thermal expansion. The non-dimensional parameters important in this problem are the Rayleigh number, $Ra = \frac{g\beta\Delta T H^3}{\nu\kappa}$, and the Prandtl number $Pr = \nu/\kappa$. With these boundary conditions convection sets in when $Ra = 1708$ for all Pr. The heat transported to the cold wall is measured in terms of the Nusselt number (Nu), which is ratio of total heat flux to the heat flux due to conduction alone. The Nusselt number is $Nu = \frac{-k\left\langle \frac{d\overline{T}}{dz} \right\rangle + \rho c \left\langle \overline{wT} \right\rangle}{k\Delta T/H}$, where k and c are the thermal conductivity and the specific heat of the fluid, w is the vertical component of fluid velocity, $\overline{\cdots}$ and $\langle \ldots \rangle$ denote temporal and horizontal averages. We consider three cases for validation:

(a) In the first case the horizontally averaged temperature profile for $Ra = 4000$ and $Pr = 0.71$ is compared with results from the numerical simulations of Lipps[11] in figure (2a).
(b) In the second case, we have compared Nu for different Ra with the results of Clever & Busse[12], who used a Galerkin method to solve for the conservation equations numerically, for $Ra = 2000$ to 50000 and $Pr = 0.71$. This is shown in figure (2b).

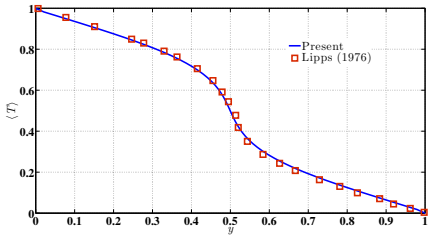

(a) Horizontally averaged temperature ($\langle T \rangle$) vs. y for $Ra = 4000$ and $Pr = 0.71$, compared with the simulations of Lipps [11]

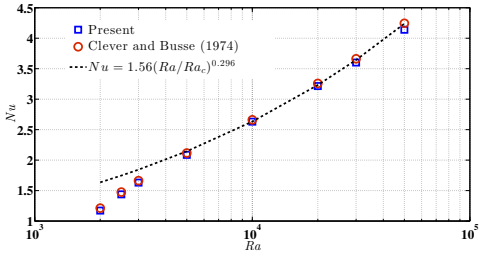

(b) Nu vs. Ra for $Pr = 0.71$, compared with the simulations of Clever & Busse [12]

Fig. 2: Validation cases for Rayleigh-Benárd convection.

(c) In the final test, we have reproduced the $Nu(Ra)$ scaling law from Johnston & Doering [13], who used a Fourier-Chebyshev spectral method to simulate Rayleigh-Bénard convection in a cell of aspect ratio of $\Gamma = 2$, defined as the ratio of length to height of the cell, and $Pr = 1$. The resolution used in their study was such that there were at least 8 grid points in the thermal boundary layers. We use the resolutions but with a uniform grid. The comparison is shown in figure (3).

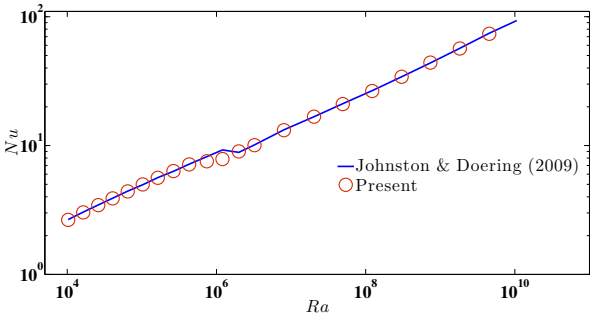

Fig. 3: Comparison of $Nu(Ra)$ with Johnston & Doering [13].

4. Results: Rayleigh-Benárd Convection against Rough Walls

1. *Periodic Roughness*

To understand the effects of roughness on thermal convection, we first use periodic roughness distributions, and describe here the validation studies that underlie a detailed examination of the associated physics [14]. Turbulent convection over pyramidal elements [15,16,17], rectangular elements [18] and V-shaped grooves [19] have been studied both experimentally and numerically. However, the specific effects of roughness on the $Nu - Ra$ scaling law differ, with some reporting a change only in the pre-factor [15,16,18], and others reporting a change both in the pre-factor and the scaling exponent [19,17]. We use a sinusoidal rough wall on the upper side of the cell. For all the cases discussed, $\Gamma = 2$ and $Pr = 1$. The periodic roughness distribution is characterized by two length scales: wavelength (λ^*) and amplitude (h^*). The amplitude $h \equiv h^*/H = 0.1$ is fixed for all cases, and two cases of $\lambda \equiv \lambda^*/H = 0.4$ and 1.0 are considered.

Figures (4a) and (4b) show the Nu-Ra scaling laws for $\lambda = 0.4$ and $\lambda = 1.0$ respectively. It is clear that introducing roughness elements influences both the pre-factor and the exponent in the scaling law. The scaling laws obtained also show that with the increase in λ, the planar case result ($Nu = 0.138 \times Ra^{0.285}$) is approached. To understand the cause for the change in the scaling law, we analyze in figures (5a) and (5b) the temperature fields for the two

cases considered. As found in the previous studies, there is enhanced plume production at the rough surface due to the interaction of the boundary layer and core flows, as seen in figure (5a). To drive this interaction, it is crucial that $h > \delta_T$, where δ_T is the thickness of the thermal boundary layer, and λ has a value from an 'optimum' range. When these conditions are met, there is an increase in the rate of heat transfer due to the plumes. However, as λ increases this interaction weakens, thereby leading to a decrease in the number of plumes produced, as seen in figure (5b).

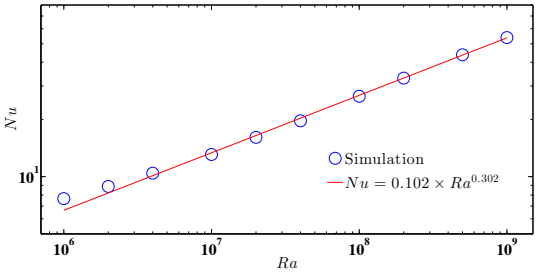

(a) *Nu-Ra* scaling law for $\lambda = 0.4$.

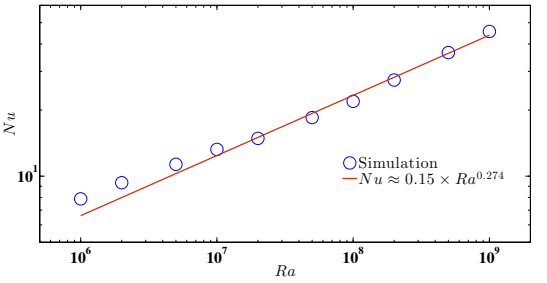

(b) *Nu-Ra* scaling law for $\lambda = 1.0$.

Fig. 4: *Nu*(*Ra*) for turbulent convection over periodic roughness distributions.

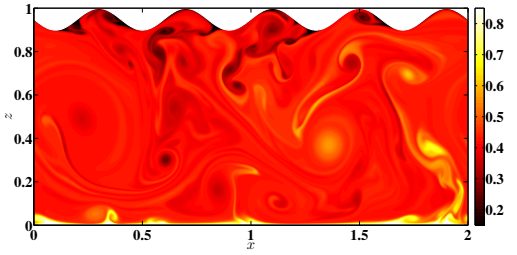

(a) Temperature field for $\lambda = 0.4$ and $Ra = 10^9$.

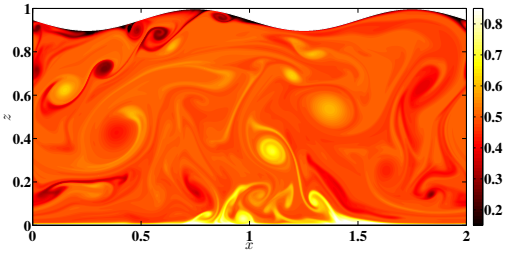

(b) Temperature field for $\lambda = 1.0$ and $Ra = 10^9$.

Fig. 5: Temperature fields over periodic roughness distributions.

2. *Random Roughness*

From the analysis of the sonar profiles of the underside of Arctic sea ice, it is found that at high wavenumbers the spectral density of roughness distribution decays as k^{-3}, where k is the wavenumber. A mathematical function having the same spectral properties as reported by Rothrock & Thorndike[20] is used to generate the rough wall for LB simulations, and is given by

$$f(x) = \sum_{k=1}^{\infty} (-p-1)^{1/2} k^{p/2} \cos(kx + \phi_k), \tag{4}$$

with $p = -3$, where ϕ_k is an independent random variable uniformly distributed in $(0, 2\pi)$.

Numerical simulations are carried out for different *Ra*, now defined based on the height of channel minus the maximum height in the roughness distribution, ranging from 2000 to 50000. Because from our validation runs, we understand the behavior of the *Nu* for these *Ra* in the smooth case, the effect of roughness on the heat transfer can be easily seen here. All simulations were carried out at $Pr = 0.71$.

Figures (6a) and (6b) show the temperature field for $Ra = 30000$ and $Ra = 50000$ respectively. The effect of the wall roughness on the cellular structures is striking and they are modified appreciably relative to the smooth-wall

cases. There are two competing effects[18]: (1) By introducing roughness one has decreased the effective *Ra*, which would result in a decrease in *Nu*; and (2) The increased area for heat transport can actually lead to an increase in *Nu*. In figure 7, the latter effect appears to dominate for the range of *Ra* considered, and there is a monotonic increase of the *Nu* with *Ra*.

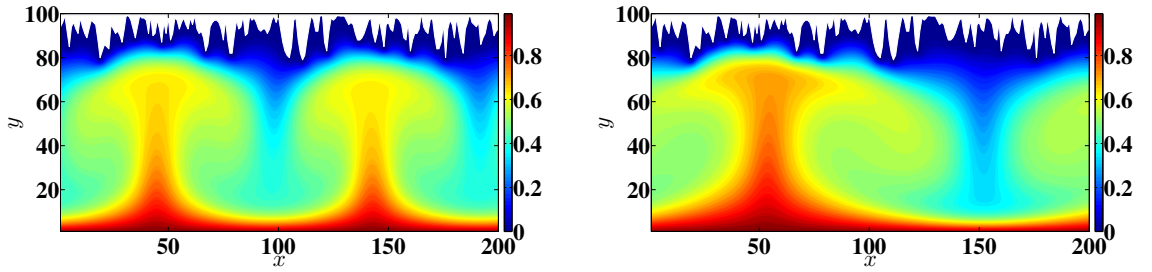

(a) Temperature field for $Ra = 30000$.

(b) Temperature field for $Ra = 50000$.

Fig. 6: Temperature field for different *Ra* and $Pr = 0.71$.

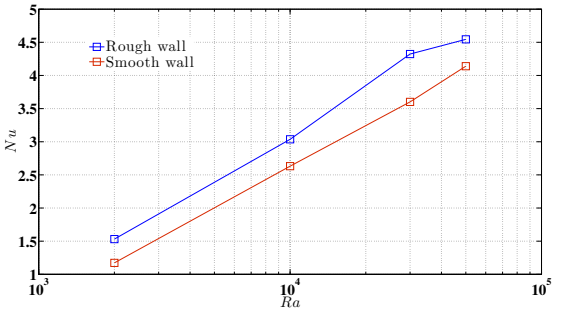

Fig. 7: *Nu* vs. *Ra* for the rough wall for $Pr = 0.71$.

5. Conclusions

A two-dimensional LB code has been developed and validated against the results in the literature for 2D channel flow and for Rayleigh-Benárd convection. The latter problem is studied with periodic and random roughness distributions on the upper side of cell. In the case of periodic rough walls, it is found that both the pre-factor and the exponent in the $Nu(Ra)$ scaling law are affected. The cause for this change is the enhanced plume production from the tips of the roughness elements. In the case of random rough walls, the large-scale flow structures are affected, and the *Nu* increased relative to the planar case. Finally, the LBM is found to be a natural way to deal with rough surfaces, because implementing the no-slip condition is easier than in traditional methods.

References

1. Kwok R, Untersteiner N. The thinning of Arctic sea ice, *Phys. Today* 2011, **64**, pp. 36-41.
2. Maykut GA, Untersteiner N. Some Results from a Time-Dependent Thermodynamic Model of Sea Ice, *J. Geophys. Res*. 1971, **76**, pp. 1550-1575.
3. M.G. McPhee, *Air-ice-ocean interaction: Turbulent ocean boundary layer exchange processes*, Springer, 2008.
4. Hultmark M, Vallikivi M, Bailey SCC, Smits AJ. Turbulent Pipe Flow at Extreme Reynolds Numbers, *Phys. Rev. Lett*. 2012, **108**.

5. Chen S, Doolen GD. Lattice Boltzmann Method for Fluid Flows, *Ann. Rev. Fluid Mech*. 1998, **30**, pp. 329 - 364.
6. Harris S, *An Introduction to the Theory of the Boltzmann Equation*, Dover Publications, 1971.
7. Succi S, *The Lattice Boltzmann Equation for Fluid Dynamics and Beyond*, Oxford Science Publications, 2001.
8. Toppaladoddi S, Wettlaufer JS, Succi S. Turbulent transport at rough surfaces. *Bulletin of the American Physical Society* **58**, (2013).
9. Monin AS, Yaglom AM. *Statistical Fluid Mechanics: Mechanics of Turbulence Volume 1*, Dover Publications, 1971.
10. Rozhdestvensky BL, Simakin IN. Secondary flows in a plane channel: their relationship and comparison with turbulent flows, *J. Fluid Mech.* 1984, **147**, pp. 261 - 289.
11. Lipps FB. Numerical Simulations of Three-dimensional Benárd Convection in Air, *J. Fluid Mech. 1976,* **75***, pp. 113 - 148.*
12. Clever RM, Busse FH. Transition to Time-dependent Convection, *J. Fluid Mech. 1974,* **65***, pp. 625 - 645.*
13. Johnston H, Doering CR. Comparison of Turbulent Thermal Convection between Conditions of Constant Temperature and Constant Flux, *Phys. Rev. Lett. 2009,* **102***, 064501.*
14. Toppaladoddi S, Succi S, Wettlaufer JS. Breaking the boundary layer symmetry in turbulent convection using wall geometry (http://arxiv.org/abs/1410.1959).
15. Du Y.-B, Tong P. Enhanced Heat Transport in Turbulent Convection over a Rough Surface, *Phys. Rev. Lett. 1998,* **81(5)**.
16. Du Y.-B, Tong P. Turbulent thermal convection in a cell with ordered rough boundaries, *J. Fluid Mech. 2000,* **407***, pp. 57 -84.*
17. Wei P, Chan T.-S, Ni R, Zhao X.-Z, Xia K.-Q. Heat transport properties of plates with smooth and rough surfaces in turbulent thermal convection, *J. Fluid Mech. 2014,* **740***, pp. 28 - 46.*
18. Shiskina O, Wagner C. Modelling the Influence of Wall Roughness on the Heat Transfer in Thermal Convection, *J. Fluid Mech. 2011,* **686***, pp. 568 - 582.*
19. Stringano G, Pascazio G, Verzicco R. Turbulent thermal convection over grooved plates, *J. Fluid Mech. 2006,* **557***, pp. 307 - 336*
20. Rothrock DA, Thorndike AS. Geometric Properties of the Underside of Sea Ice, *J. Geophys. Res*. 1980, **85**, pp. 3955-3963.